A hybrid photovoltaic power converter system for Brushless DC Motor operation and Control

Visvanathan K

[1]*Research scholar, Department of EEE, North East Frontier Technical University, Sipu Puyi, Aalo (P.O), Arunachal Pradesh,*

Email: visvanathanphd16@gmail.com

Dr. SANJAY S CHAUDHARY

[2]*Professor, Department of EEE, Maharishi University Of Information Technology, Sitapur Road, P.O. Maharishi Vidya Mandir, Lucknow, Uttar Pradesh 226013,*

Abstract

In the growth of renewable generation system, photovoltaic power generation plays an important role in present era. This paper presented an effective hybrid photovoltaic power generation using hybrid Cuk-Sepic power converter in integrated form. The space vector based neuro fuzzy sensor-less control is presented for brushless DC motor in variable load operation and control. Motor drawn supply power from hybrid photovoltaic generation. A fuzzy logic based MPPT scheme is applied for hybrid photovoltaic converter to extract maximum power. This presented configuration is used to an efficient power sharing of two- photovoltaic power generation to meet out power demand on load. The system was tested under high load brushless DC motor and dump load to verify hybrid power generation capacity. The circuit was tested using MATLAB/Simulink software to verify about this control and circuit configuration.

Index terms: PV (Photovoltaic system), Two-diode PV system, MPPT (Maximum Power Point Tracking), Fuzzy MPPT (Fuzzy based IC), hybrid Cuk-Sepic converter, VSI (Voltage Source Inverter), Sensor-Less Vector Control

I. Introduction

In fast growing of renewable generation, photovoltaic system is in notable part of power generation. The unique merits and reason for choosing a photovoltaic system, pollution free in nature, noiseless power generation, low maintenance and etc. multiple power system used for power generation for supplying grid power [1]-[5]. A hybrid converter scheme is having merits such as continuous power flow, integration of two areas of power generation and high power generation [6]. Even it has so many merits but it suffering by component extraction, maintenance

requirement, Reverse power flow problem and low efficiency. So modified scheme was introduces in hybrid converter circuit to meet out drawbacks of conventional system [7]. This modified form of Cuk-Sepic converter is used to sharing of two-generation power in effective manner.

The two diode scheme is implemented in photovoltaic system for increasing efficiency, processing of iteration speed and reducing of computation time while comparison with single diode based photovoltaic system [8], [9]. The topology is proposed that two diode photovoltaic system with having high efficiency, simplified structure and neglecting series/ parallel resistor. Photovoltaic performance and its characteristic is varied by temperature variation, solar irradiation and output power so parameters of saturation current(I_0), series resistance(R_S), shunt resistance(R_{SH}), photovoltaic current (I_{PV}) and ideality constant(A). A maximum power point tracking is introduces to extract power from photovoltaic system by varying condition of irradiation and temperatures. A fuzzy logic based MPPT (Maximum Power Point Tracking) is presented for proposed two-diode photovoltaic system. This is modified form of incremental conductance scheme and reached high power extraction over classical MPPT topology.

This paper is presented the hybrid cuk-sepic photovoltaic converter is applied for low to high load BLDC (Brush Less DC) Motor Control. Fuzzy logic based MPPT scheme is used to extract maximum power from two-area of photovoltaic power generation using Cuk-Sepic converter. Two-diode photovoltaic equivalent circuit is introduces to reduces commutation time and efficiency in photovoltaic generation. An aim of hybrid cuk-sepic converter to provide continuous power, high efficient power sharing and generate a maximum power to load. Brushless DC motor is undergone in various load condition for proposed power generation circuit configuration. A neuro-fuzzy logic based vector control scheme is used to control of torque, speed and stator current performance for wide load variation. The system was tested using MATLAB/Simulink software to analysis about performances
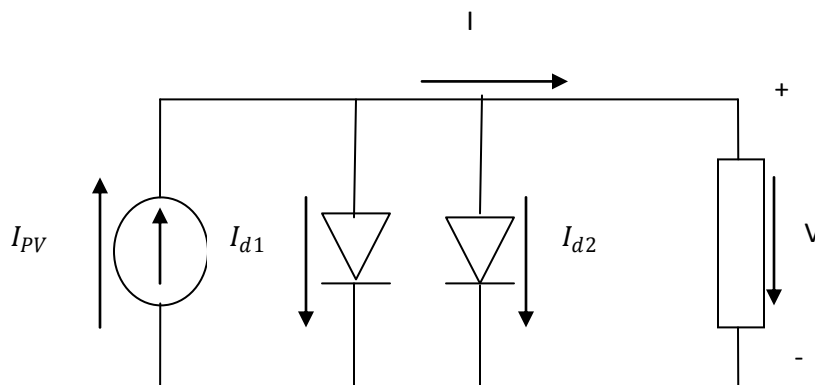
Photovoltaic system

Fig. 1 equivalent circuit for two diode photovoltaic system

From the Fig.1, two-diode model the current equation can be represented in equation (1) accordingly;

$$I = I_{PV} - \left[\exp\left(\frac{q(V+IR_S)}{N_S KTA_1}\right) - 1\right] - I_{02}\left[\exp\left(\frac{q(V+IR_S)}{N_S KTA_2}\right) - 1\right] - (V + IR_S)/R_{sh} \qquad (1)$$

Where

q - Electron charge ($1.6 \times 10{-}19$C)

K - Boltzmann constant ($1.38 \times 10{-}23$Nm/K)

T- PV module temperature in Kelvin

I_{01} - reverse saturation current of diode 1

I_{02} - reverse saturation current of diode 2

A_1 -diode ideality constant of diode 1

A_2 - Diode ideality constant of diode 2

I_{PV} - Light generated current of PV module in amperes

R_s -series resistance of PV module

R_{sh} -parallel resistance of PV module

N_s - Number of PV cells connected in series.

I- PV current (A).

A mathematical model of the PV module is constructed by using five parameters, such as reverse saturation current (I_0), photoelectric current (I_{PV}), series resistance (R_s), shunt resistance (R_{sh}), and ideality constant (A), are required to be calculated its magnitude of I_{02} is found that nonlinear equations (5) and some of the parameters are assumed arbitrarily, since required to reduce the number of unknowns. A two diode model is attempt to reduce mathematical computation time and complexity, the proposed model has reduces the series and parallel resistances [10]

$$I = I_{PV} - I_{01}\left[\exp\left(\frac{q(V)}{N_S KTA_1}\right) - 1\right] - I_{02}\left[\exp\left(\frac{q(V)}{N_S KTA_2}\right) - 1\right] \qquad (2)$$

I_{PV} , I_{01} , I_{02} , A_1 , A_2 are unknown parameters to be found in pv model respectively. I_{02} is derived from I_{01} ; however the further unknown parameters are estimated. Those are determined from the constructed datasheet, which is obtained below. PV current (I_{PV}) can be derived from in terms of a short-circuit current under well standard test conditions (STC) in which the PV cell surface irradiation and temperature are 900W/m2 and 300 K by (3), consider variation of temperature and irradiation. I_{PV} Has a linear relationship to irradiation (G) and short-circuit current (I_{sc}) [11], and which can be follows as

$$I_{PV} = (I_{SC} + K_I \Delta T) \frac{G}{G_{STC}} \tag{3}$$

Where I_{SC} is the short-circuit current under STC, ΔT is the temperature difference between module temperature (T) and the STC temperature, K_I is called short-circuit current constant and this is preferred from the datasheet, G is surface irradiation, and GSTC is the surface irradiation under short-circuit current. The equation to describe the saturation current is taken by

$$I_{01} = \frac{(I_{sc} + K_I \Delta T)}{\exp\left[(V_{oc} + K_v \Delta T) * \frac{q}{(N_S K T A_1)}\right] - 1} \tag{4}$$

Where K_v is called voltage temperature constant and the value is taken from data sheet, and V_{oc} is the open-circuit voltage. it can be describes as equation (5)

$$I_{02} = \left(\frac{T^{\frac{2}{5}}}{3.77}\right) I_{01} \tag{5}$$

Finally find A_1, A_2 values by using simple and fast iterative method, by following two conditions are considered:

a) open-circuit condition with V_{oc} ;

b) Maximum power point (MPP) condition with V_m and I_m.

Under open-circuit condition, $V = V_{oc}$, $I = I_{oc} = 0$; $V = V_{oc}$

$$0 = \left|I_{PV} - I_{01}\left[\exp\left(\frac{q(V_{oc})}{N_S K T A_1}\right) - 1\right] - I_{02}\left[\exp\left(\frac{q(V_{oc})}{N_S K T A_2}\right) - 1\right]\right| \tag{6}$$

A_2 Can be obtained from A_1 ,

$$A_2 = \frac{(qV_{oc})}{N_S TK \ln\left(\frac{I_{PV} - I_{01}\left(\exp\left(qV / (N_S K T A_1 T)\right) - 1\right)}{I_{02}} + 1\right)} \tag{7}$$

At high voltage condition the single diode equation assumes a constant value for the ideality factor. But the two diode estimation of ideality constants A_1 and A_2 varied based on the iterative matching algorithm. The calculated ideality values A_1 and A_2 for the PV modeling matching algorithm is given [12]. The amount of photovoltaic power extraction is drawn from proposed two photovoltaic system is obtained by fuzzy logic based MPPT controller. It is a modified form of incremental conductance scheme so it can able to control for delivering power continuously.

II.   Hybrid Cuk-Sepic converter topology

The present configuration of hybrid photovoltaic converter is the combined circuit topology of cuk-SEPIC Converter which is shown in Fig.1. SPEIC circuit is fed with photovoltaic system1. Cuk circuit is fed with photovoltaic system 2. Proposed approach is unique power flow structure which Compared with conventional hybrid circuit topology [13]. The enhancement of this approach is reduced number of switches by moderate hybrid structure. Inductor $(L2)$ and filter capacitor $(C0)$ are used as common elements for both Cuk and SEPIC converters of operation. The detailed power flow circuit and explanations are given bellow.
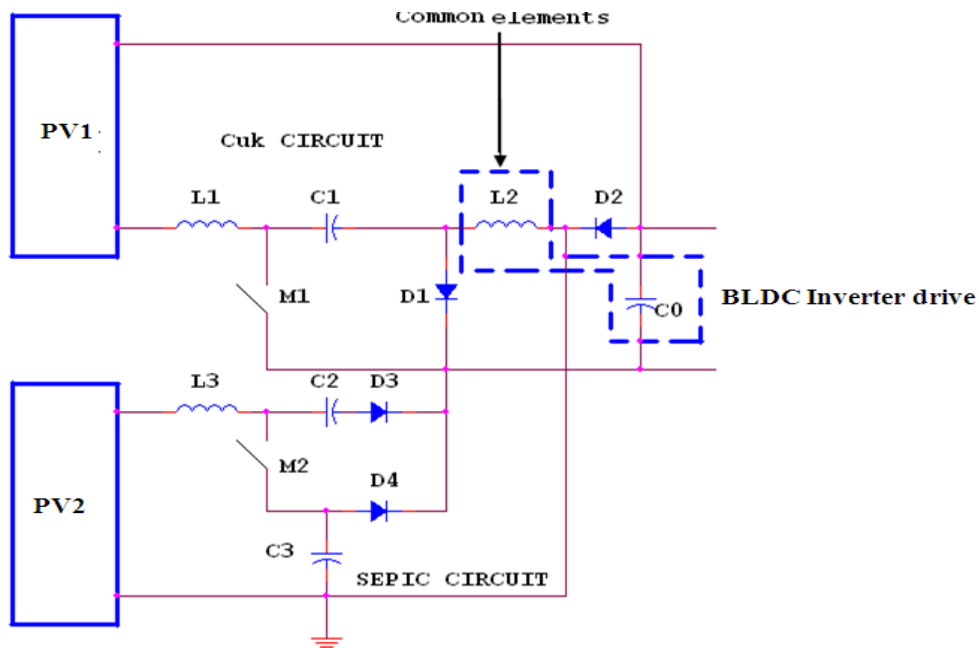

Fig.2 Moderate Hybrid Converter Using Cuk-SEPIC

Mode 1:

During initial mode (T_0-T_1) of proposed circuit is drawn power by conduction of M1 and M2 switch shown in Fig.3. Charged inductor (L1), (L2) and capacitor (C1) is discharging to filter or load capacitor (C0). During time interval in SEPIC circuit, charged inductor (L3), capacitor (C2) is drawn power from photovoltaic and delivered to load capacitor (C0). capacitor (C0) is drawn maximum power from photovoltaic system 1 and photovoltaic system 2 .
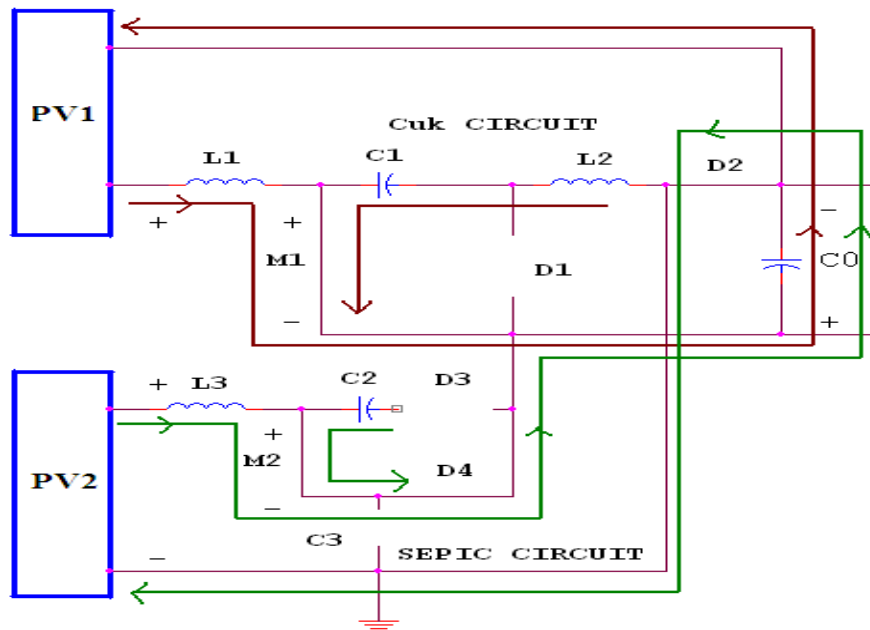

Fig. 3 Mode 1 power flow circuit when Both M1 and M2 ON

Mode 2:

During second mode (T1-T2) of proposed circuit is drawn power by conduction of M1 and non-conduction of M2 switch shown in Fig.4. Cuk converter circuit behaves as it is mentioned mode1 and secondary circuit of SEPIC circuit draws power from PV-2 through (L3), (D3) to load capacitor (C0). During this mode, reverse flow of current (Id) and (IC) current is drawn to

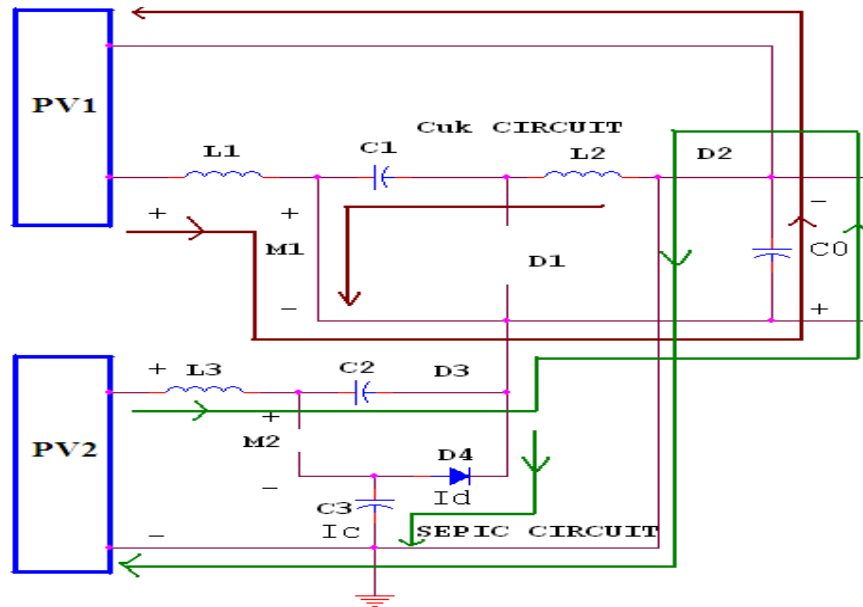ground while (D2) is conduct. This moderate circuit is used to drawn power from both generations to load.

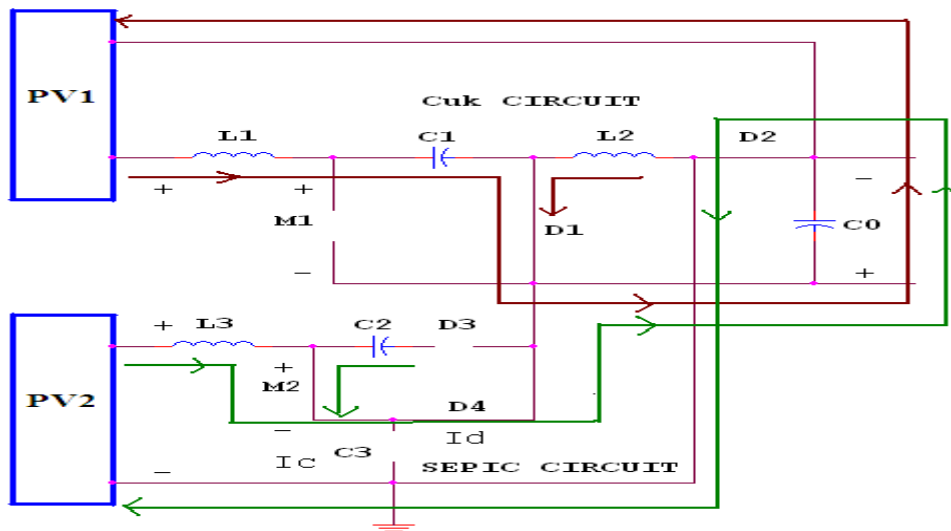Fig.4 Mode 2 Power flow circuit when M1 ON and M2 OFF

Mode 3:

Fig.5 Mode 3 power flow when M1OFF and M2 ON

During third mode (T_2-T_3) of proposed circuit configuration is drawn power by conduction of M2 and non-conduction M1 shown in Fig.5. Cuk circuit is draws power form phtovoltaic system-1 through (L1) and (C1) to load capacitor (C0) via D1. Secondary circuit of SEPIC converter is drawn power from Photovoltaic system 2 through (L3), (C2) to filter capacitor (C0). Load drawn power simultaneously at equal time interval. Already charged energy across (C2) is also delivering power to load through (M2). The delivering power in circuit is depends on amount of generation on photovoltaic side
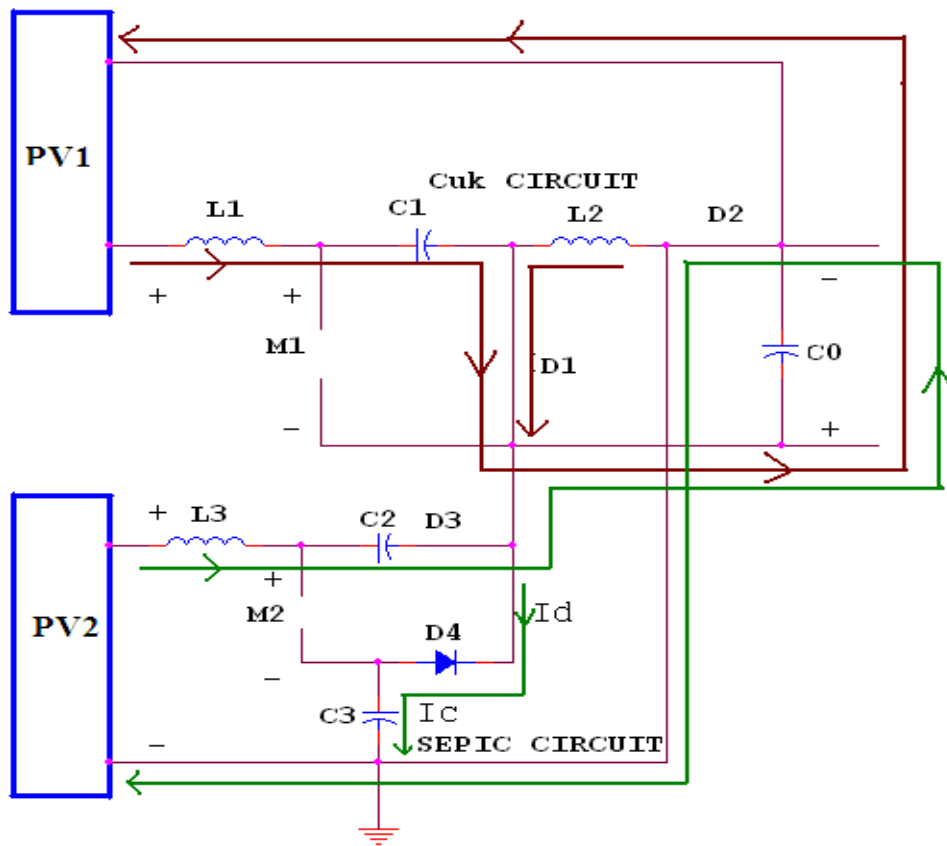
Mode 4

Fig.6 Mode 3 power flow when M1OFF and M2 ON

During fourth mode (T3-T4) of proposed circuit configuration is drawn power from both photovoltaic generation by non-conduction of M1 and M2 is shown in Fig.6. Photovoltaic system-1 generated power in Cuk is passed through inductor circuit across (L1), capacitor (C1) and also energy stored across (L2) is delivered in same path of (D1) to (C0). Photovoltaic power generation-2 in SEPIC converter, power passed through (L3) and (C2) to load side filter (C0) and

reached ground through diode (D1). At the same time of operation, reverse current (Id) across diode (D4) and current (IC) across capacitor (C3) flows to ground.

The analysis of fours modes of operation is clearly shows that load drawn power from each generation (both photovoltaic system-1 and photovoltaic system-2) is obtained regularly and effective power generation is entered to load in every modes of operation. This is the unique flow circuit over conventional hybrid system. The efficiency of proposed configuration is verified for wide load variation and control of brushless DC Motor

III.   Control of Brushless DC Motor using Vector control topology

The presented voltage source inverter controller is generating reference signals by comparing with positive sequence of supply voltage with load voltages is shown in Fig.7 Supply voltage (V_{ia}, V_{ib}, V_{ic}) is transformed as $(d - q - 0)$ using transformation method as given by equation (8) and (9).

$$Trans = \sqrt{2/3} \begin{bmatrix} 1/\sqrt{2} & 1/\sqrt{2} & 1/\sqrt{2} \\ sin(\omega t) & sin(\omega t - 2\pi/3) & sin(\omega t + 2\pi/3) \\ cos(\omega t) & cos(\omega t - 2\pi/3) & cos(\omega t + 2\pi/3) \end{bmatrix} \qquad (8)$$

$$Trans^- = \sqrt{2/3} \begin{bmatrix} 1/\sqrt{2} & sin(\omega t) & cos(\omega t) \\ 1/\sqrt{2} & sin(\omega t - 2\pi/3) & cos(\omega t - 2\pi/3) \\ 1/\sqrt{2} & sin(\omega t + 2\pi/3) & cos(\omega t + 2\pi/3) \end{bmatrix} \qquad (9)$$

$$\begin{bmatrix} V_{i0} \\ V_{id} \\ V_{iq} \end{bmatrix} = Trans \begin{bmatrix} V_{ia} \\ V_{ib} \\ V_{ic} \end{bmatrix} \qquad (10)$$
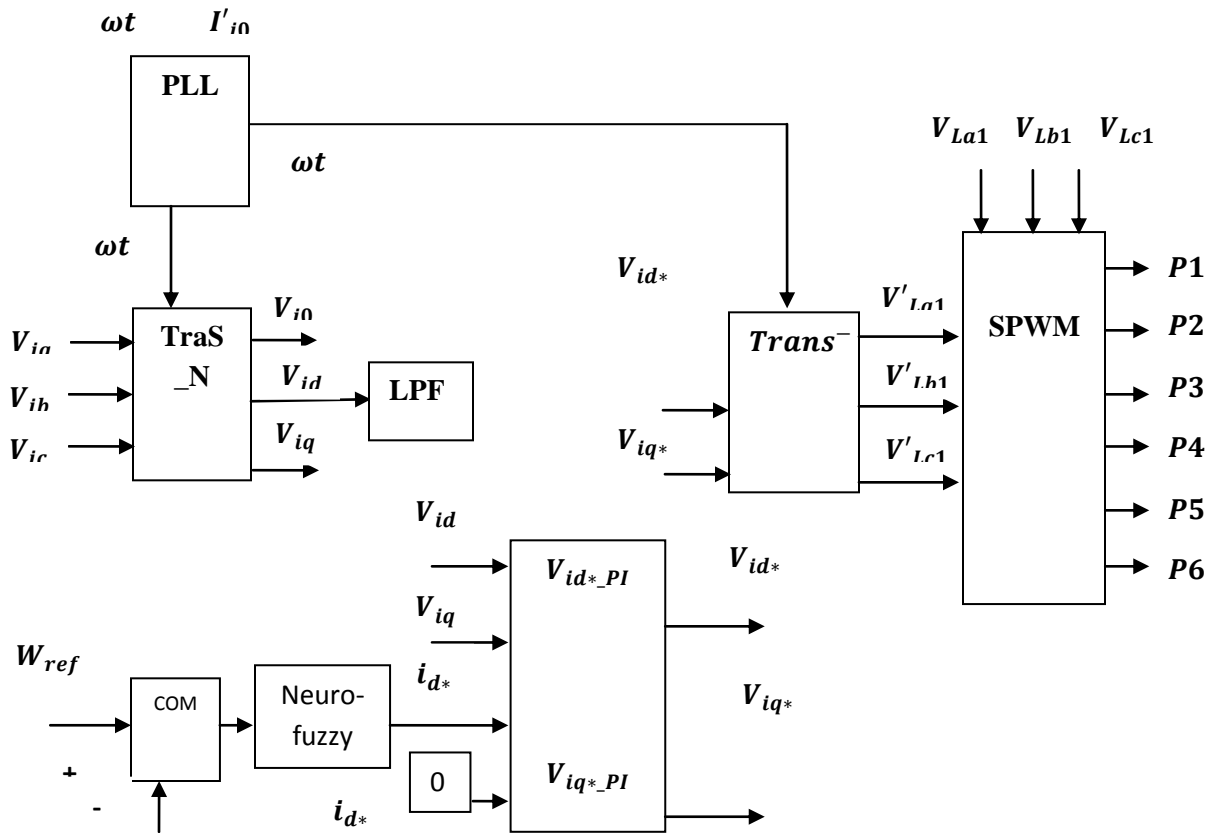
Fig.7 Proposed controller circuit diagram using neuro-fuzzy vector controller

A rapid voltage V_{id}, V_{iq} is having both oscillation elements $\tilde{V}_{id}, \tilde{V}_{iq}$ and mean elements $\overline{V}_{id}, \overline{V}_{iq}$ with respect to unbalancing utility grid supply and harmonics condition. The same rapid voltage V_{id}, V_{iq} is having negative sequence components and harmonics occurrences on distorted supply voltage conditioS_N. Positive sequence is occurs on mean value of elements and zero sequence is occur on unbalancing voltage condition. One of rapid voltages $\boldsymbol{V_{id}}$ is consists of mean value and oscillation components is given by

$$V_{id} = \tilde{V}_{id} + \overline{V}_{id} \tag{11}$$

The reference voltages on load side $(V_{La1b1c1})$ are calculated is given by

$$\begin{bmatrix} V'_{La1} \\ V'_{Lb1} \\ V'_{Lc1} \end{bmatrix} = Trans^- \begin{bmatrix} \overline{V}_{i0} \\ \overline{V}_{id} \\ \overline{V}_{iq} \end{bmatrix} \tag{12}$$

Inverse transform calculation is applying by mean components across supply voltage and ωt in proposed speed based vector control. Direct axis of positive sequence components voltages is

calculated by low pass filters which is presented on controller circuit is shown in Fig.7. In equation (10), zero sequence components and negative sequence components becomes zero for control and overcoming an unbalancing, distorted and harmonics on system. A sinusoidal pulse width modulation is generated by comparing generated reference signals $V'_{La1,Lb1,Lc1}$ with load voltage $V_{La1,Lb1,Lc1}$.

Direct axis references current is calculating by comparing reference speed (ω_{ref}) and actual speed (ω_{act}) and given to speed control (neuro fuzzy logic control) to smooth and eliminate peak overshoot and gives a controlled direct axis current (i_{d*}) as an output. The output waveform is described by following mechanical equation

$$\frac{d\omega_r}{dt} = \frac{1}{j}(T_e - T_m - B\omega_r)$$

Where, j is inertia of motor, B is viscous coefficient, T_m is a mechanical and T_e is an electrical torque.

IV. Space vector pulse width modulation

A simple space vector based pulse width modulation scheme is introduces for controlling IBGT on inverter using reference voltage generation is shown in Fig.8 can be represented by switching states. Switching states are defined by torque error and flux errors shown in Table-1 and Table-2.

Table I. Switching State for proposed inverter configuration

state	Leg A			Leg B			Leg C		
	S_1	S_4	V_{an}	S_3	S_6	V_{bn}	S_5	S_2	V_{cn}
1	on	off	V_d	on	off	V_d	on	off	V_d
0	off	on	0	off	on	0	off	on	0

Table II. Switching State for proposed inverter configuration

Space vector		Switching state (three phases)	ON-state switch	Definition
Zero vector	$\vec{V}_1$	[1 1 1]	S_1, S_3, S_5	0
		[0 0 0]	S_4, S_6, S_2	
Active vector	$\vec{V}_2$	[1 0 0]	S_1, S_6, S_2	$\vec{V}_1 = \frac{2}{3} V_d e^{j0}$
	$\vec{V}_3$	[1 1 0]	S_1, S_3, S_2	$\vec{V}_1 = \frac{2}{3} V_d e^{j\frac{\pi}{3}}$
	$\vec{V}_4$	[0 1 0]	S_4, S_3, S_2	$\vec{V}_1 = \frac{2}{3} V_d e^{j\frac{2\pi}{3}}$
	$\vec{V}_5$	[0 1 1]	S_4, S_3, S_5	$\vec{V}_1 = \frac{2}{3} V_d e^{j\frac{3\pi}{3}}$
	$\vec{V}_6$	[0 0 1]	S_4, S_6, S_5	$\vec{V}_1 = \frac{2}{3} V_d e^{j\frac{4\pi}{3}}$
	$\vec{V}_7$	[1 0 1]	S_1, S_6, S_5	$\vec{V}_1 = \frac{2}{3} V_d e^{j\frac{5\pi}{3}}$

Voltage state is derived from α and β reference frame below.

$$\vec{V}_{ref} = V_\alpha + jV_\beta = \frac{2}{3}(V_a + aV_b + a^2 V_c) \tag{18}$$

Similarly,

$$|\vec{V}_{ref}| = \sqrt{V_\alpha^2 + V_\beta^2}, \qquad \alpha = \tan^{-1}\left(\frac{V_\beta}{V_\alpha}\right)$$

$$V_\alpha + jV_\beta = \frac{2}{3}\left(V_a + e^{j\frac{2\pi}{3}}V_b + e^{-j\frac{2\pi}{3}}V_c\right) \tag{19}$$

$$V_\alpha + jV_\beta = \frac{2}{3}\left(V_a + \cos\frac{2\pi}{3}V_b + V_a + \cos\frac{2\pi}{3}V_c\right) +$$

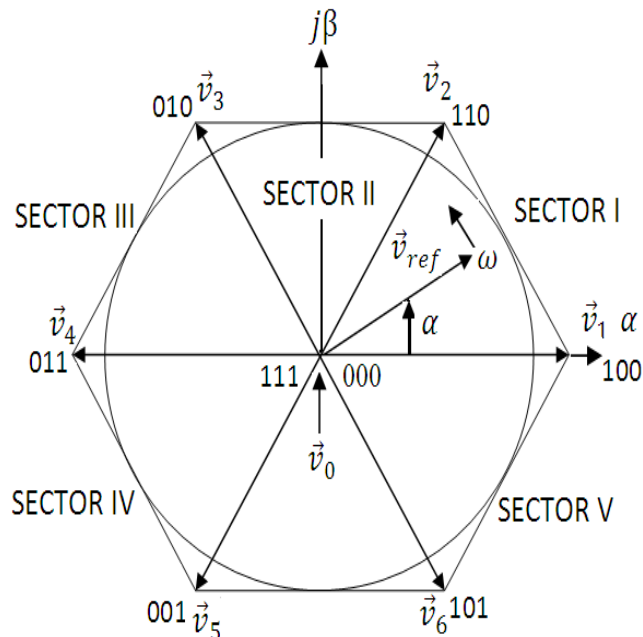$$j\frac{2}{3}\left(\sin\frac{2\pi}{3}V_b - \sin\frac{2}{3}V_c\right) \tag{20}$$

Fig. 8. Space vector diagram for two level inverter

By equating the real and imaginary parts derived by,

$$V_\alpha = \frac{2}{3}(V_a + \cos\frac{2\pi}{3}V_b + \cos\frac{2\pi}{3}V_c$$

$$V_\beta = \frac{2}{3}\left(0V_a + \sin\frac{2\pi}{3}V_b - \sin\frac{2\pi}{3}V_c\right)$$

$$\begin{bmatrix} V_d \\ V_q \end{bmatrix} = \frac{2}{3}\begin{bmatrix} 1 & \cos\frac{2\pi}{3} & \cos\frac{2\pi}{3} \\ 0 & \sin\frac{2\pi}{3} & \sin\frac{2\pi}{3} \end{bmatrix} \cdot \begin{bmatrix} V_a \\ V_b \\ V_c \end{bmatrix} \qquad (21)$$

The proposal of space vector modulation used to improved brushless DC Motor performances such as speed and current via neuro- fuzzy based vector control loop. Space vector modulation is interacting with vector control loop which phase lock loop circuit, park transform/park inverse transform, speed regulator using neuro fuzzy logic controller.

V. Simulation result

The presented scheme of hybrid photovoltaic system is generating in effective manner using Cuk-Sepic Converter. Hybrid converter performance is improved by fuzzy logic based MPPT scheme. The proposed power generation is applied for brushless DC Motor operation and control of brushless dc motor is obtained by space vector based vector control using neuro fuzzy logic controller. Brushless DC Motor is undergone for wide load variation test for proposed Hybrid photovoltaic converter. The photovoltaic system parameters design is implemented using Table

III, parameters of presented system configuration is presented using Table IV and motor configuration is used in Table V.

Table III parameters for Two-Diode photovoltaic system

Kyocera KC200GT for Two-Diode photovoltaic system	
Parameters	Value
$I_{sc}(A)$	8.20
$V_{oc}(V)$	32.90
$I_{mp}(A)$	7.61
$V_{mp}(V)$	26.3
$I_{o1}(A)$	5.0122×10^{-4}
$I_{o2}(A)$	1.298×10^{-5}
$I_{PV}(A)$	17
A1	1.7
A2	2.5

The two-diode photovoltaic system is designed using parameters given in Table III for applying voltage source inverter as an input supply via buck-boost converter system. Proposed system is designed using parameters given in Table IV and motor parameters used for presented scheme is given in Table V.

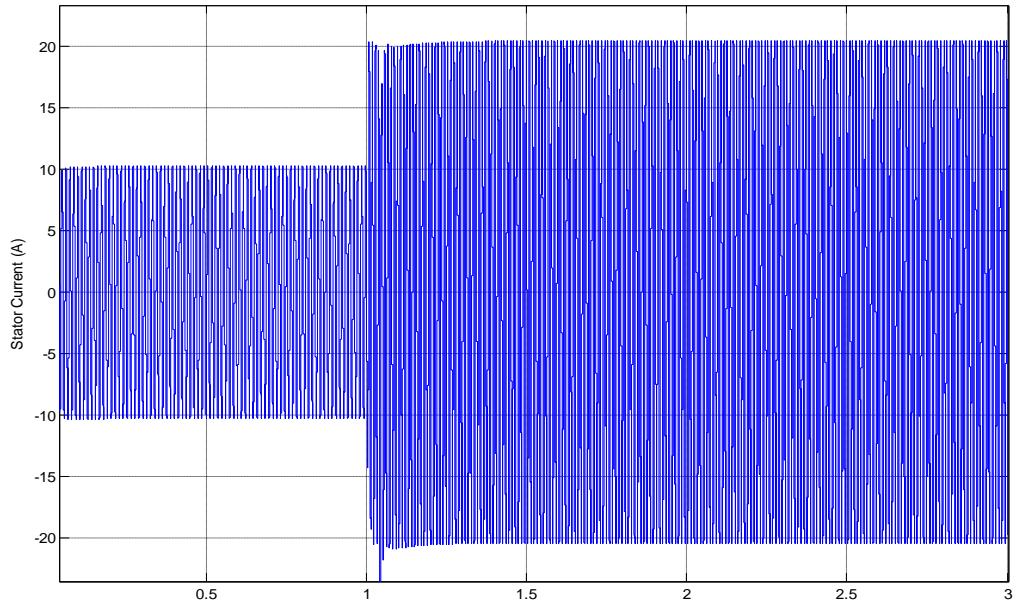Table IV Parameters for proposed system

Parameters	Value
PV (V)	200
$MPPT$ (V)	600
$INV(V)AC$	600
Inverter frequency (f)	1kHz
$Load\ power$	500W

L1	$128\mu H$
L2	$58\mu H$
L3	$108\mu H$
C1	$755\mu F$
C2	$1808\mu F$
C3	$400\mu H$
C0	$407\mu H$
Buck-boost converter frequency (f)	25kHz

Table V Parameters for BLDC Motor

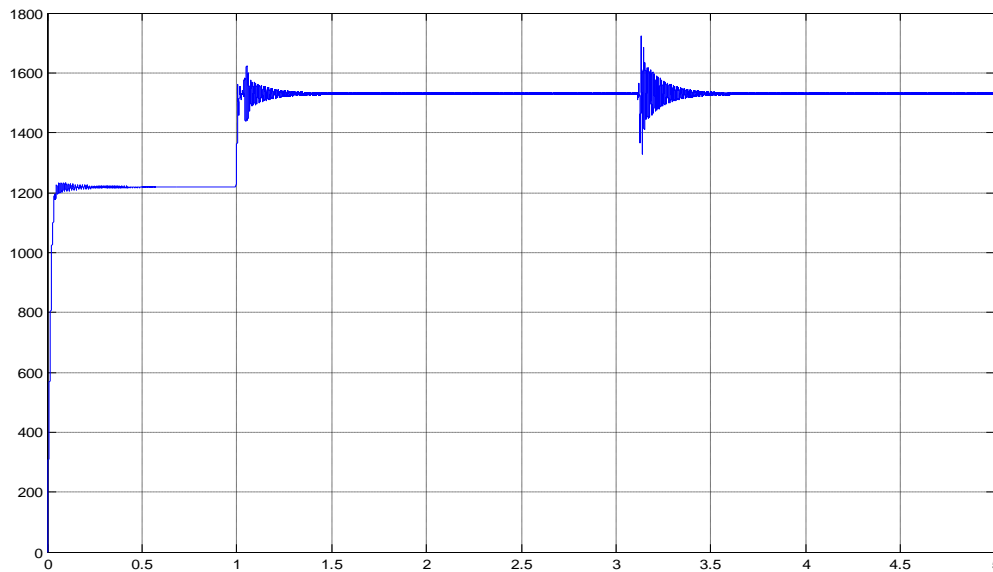| Parameters	Value
Nominal Power (W)	200
Voltage (V)	600
Frequency (f)	600
R_s	2.8750Ω
L_s	8.5mΩ
Rotor flux linkage	0.18Wb
P_P	4
J	0.0008 $kg.m^2$

The brushless DC Motor is tested for wide load variation from low to high at 1sec and also speed, current and torque performances are obtained in desired level even at load variation. Implementation circuit is shown in Fig.9, proposed hybrid converter and motor performances are achieved in Fig.10 and Fig.11.

Fig.9 simulation implementation circuit for proposed configuration

(a)

(b)

Fig.10 simulation implementation circuit for proposed configuration

(a)
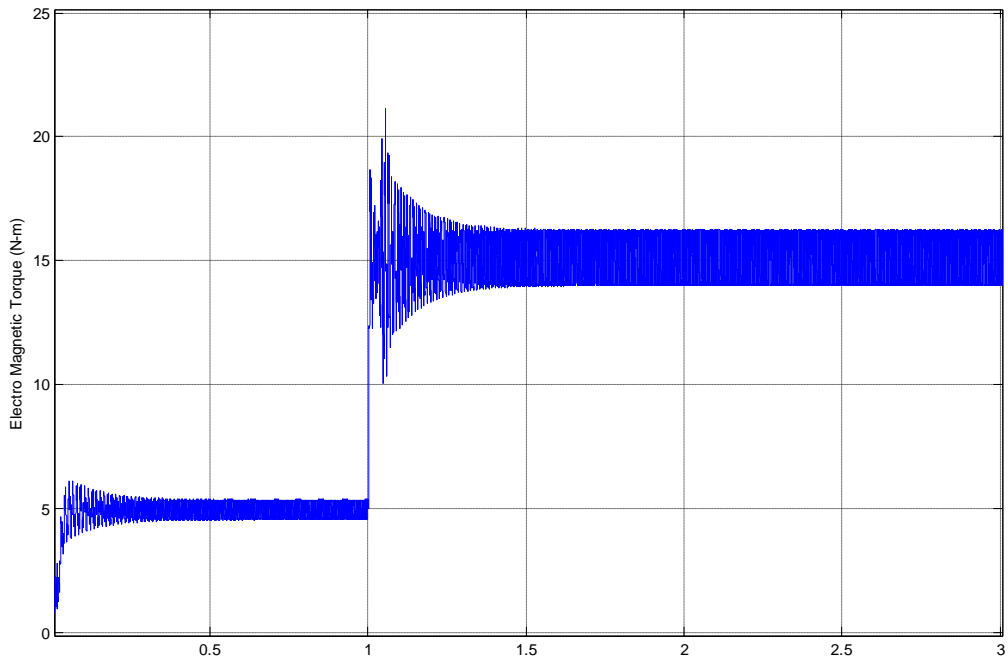
(b)

(c)

Fig.11 simulation implementation circuit for proposed configuration

VI. Conclusion

The enhancement of this approach provides an efficient power sharing from photovoltaic power system using cuk-sepic converter and power generation performance is improved by proposed fuzzy logic based MPPT control scheme. The neuro -fuzzy logic based vector control is greatly control brushless DC Motor control so that this can capable of speed and torque control for wide range of speed application. This paper introduces an efficient power generation and speed-torque control of brushless DC Motor using simple space vector modulation based neuro-fuzzy vector control scheme. An electromagnetic torque and speed performances is maintained in constant even at high load and low load conditions. The simulation implementation was carried out to verify the performances of proposed configuration using MATLAB/Simulink software and proved their performances in photovoltaic generation and motor performance.

References

1. Matsuo, H. "Novel Solar Cell Power Supply System using the Multiple-input DC-DC Converter; Telecommunications Energy Conference, 1998; INTELEC." In 20th International, pp. 797-8022.
2. Amirabadi, Mahshid, Hamid A. Toliyat, and William C. Alexander. "A multiport AC link PV inverter with reduced size and weight for stand-alone application." IEEE Transactions on Industry Applications vol.49. no.5, 2013, pp.2217-2228.

3. Zhao, Chuanhong, Simon D. Round, and Johann W. Kolar. "An isolated three-port bidirectional DC-DC converter with decoupled power flow management." IEEE Transactions on Power Electronics 23.5 (2008): 2443-2453.

4. Carrasco, J. M., Franquelo, L. G., Bialasiewicz, J. T., Galván, E., PortilloGuisado, R. C., Prats, M. M & Moreno-Alfonso, N. "Power-electronic systems for the grid integration of renewable energy sources: A survey " IEEE Transactions on industrial electronics, vol.53, no.4, 2006, pp.1002-1016.

5. Zhao, Chuanhong, Simon D. Round, and Johann W. Kolar. "An isolated three-port bidirectional DC-DC converter with decoupled power flow management." IEEE Transactions on Power Electronics, vol.23, no.5, 2008, pp.2443-2453.

6. S.K. Kim, J.H Jeon, C.H. Cho, J.B. Ahn, and S.H. Kwon, "Dynamic Modeling and Control of a Grid-Connected Hybrid Generation System with Versatile Power Transfer," IEEE Transactions on Industrial Electronics, vol. 55, pp. 1677-1688, April 2008.

7. Hui, Joanne, Alireza Bakhshai, and Praveen K. Jain. "A hybrid wind-solar energy system: A new rectifier stage topology." Applied Power Electronics Conference and Exposition (APEC), 2010 Twenty-Fifth Annual IEEE. IEEE, 2010.

8. Babu, B. C., & Gurjar, S. (2014) "A novel simplified two-diode model of photovoltaic (PV) module" Photovoltaics, IEEE Journal of, 4(4), 1156-1161.

9. Salam, Z., Ishaque, K and Taheri, H. (2010, December) "An improved two-diode photovoltaic (PV) model for PV system," in Proc. Joint Int. Conf. Power Electron., Drives Energy Syst.,New Delhi, India, Dec. 2010, pp. 1–5

10. Y. Mahmoud, W. Xiao, and H. H. Zeineldin, "A simple approach to modelling and simulation of photovoltaic modules," IEEE Trans. Sustainable Energy, vol. 3, no. 1, pp. 185–186, Jan. 2012.

11. S. Liu and R. A. Dougal, "Dynamic multiphysics model for solar array,"IEEE Trans. Energy Convers., vol. 17, no. 2, pp. 285–294, Jun. 2002

12. Babu, B. C., & Gurjar, S. (2014) "A novel simplified two-diode model of photovoltaic (PV) module" Photovoltaics, IEEE Journal of, 4(4), 1156-1161.

13. Hui, Joanne, Alireza Bakhshai, and Praveen K. Jain. "A hybrid wind-solar energy system: A new rectifier stage topology." Applied Power Electronics Conference and Exposition (APEC), 2010 Twenty-Fifth Annual IEEE, pp. 155-161, Feb.2010